

# Novel Microwave-Assisted Solution-Phase Approach to Radial Arrays Composed of Prismatic Antimony Trisulfide Whiskers

Hui Wang,<sup>†</sup> Jian-Min Zhu,<sup>‡</sup> Jun-Jie Zhu,<sup>\*,†</sup>  
Li-Min Yuan,<sup>§</sup> and Hong-Yuan Chen<sup>†</sup>

State Key Laboratory of Coordination Chemistry,  
Department of Chemistry, and National Laboratory of Solid  
State of Microstructures, Nanjing University,  
Nanjing 210093, China, and Testing Center,  
Yangzhou University, Yangzhou 225009, China

Received July 2, 2003. In Final Form: September 28, 2003

## Introduction

Dimensionality plays a critical role in determining the properties of materials due to, for example, the different ways that electrons interact in three-dimensional (3D), two-dimensional (2D), and one-dimensional (1D) structures.<sup>1</sup> Over the past decade, submicrometer- and nanometer-scale 1D structural materials have stimulated increasing interest as a result of their great importance in both basic scientific research and potential technological applications.<sup>2</sup> An important issue in the study and application of these 1D materials is how to rationally assemble atoms or other building blocks into anisotropic 1D structures with small-sized diameters (in the nanometer or submicrometer scale) but much longer lengths (up to over several micrometers) in an effective and controllable way. Although solid-state materials with submicrometer or nanoscale 1D structures can be fabricated by advanced lithographic techniques<sup>3</sup> or via gas-phase chemical processes,<sup>4</sup> solution-phase chemical synthesis is regarded as a more promising approach in terms of much lower cost and potential for high-volume production as well as tight dimension control. Among the solution-phase approaches that have already been reported, template directed<sup>5</sup> or crystal seed mediated methods<sup>6</sup> are most

commonly employed to confine or catalyze the preferential 1D growth of various kinds of materials. However, exploring convenient and efficient solution-phase approaches to 1D structural materials without using any templates or crystal seeds still remains a great challenge.

Another major scientific challenge in 1D material research is to develop simple and efficient methods to create the patterns of well-arranged 1D structural materials in a predictable and controllable way. One possible route is to develop suitable hierarchical assembly techniques to put 1D structural building blocks together into functional structures.<sup>2d</sup> The other possibility, which is more convenient and, thus, more attractive, is to form superstructural arrays through direct one-step growth processes.

Antimony trisulfide ( $\text{Sb}_2\text{S}_3$ ) is a representative V–VI group binary chalcogenide that has wide applications in target materials for television cameras, microwave switching, solar energy conversion, and various optoelectric devices.<sup>7</sup>  $\text{Sb}_2\text{S}_3$  is a highly anisotropic V–VI group semiconductor with a layered structure parallel to the growth direction and crystallizes in an orthorhombic phase.<sup>8</sup> In the past two decades, a variety of experimental approaches have been established to prepare  $\text{Sb}_2\text{S}_3$ , in the form of either solid thin films<sup>7,9</sup> or ultrafine powders.<sup>10</sup> Herein, we develop a solution-phase growth method to fabricate radial arrays composed of prismatic  $\text{Sb}_2\text{S}_3$  whiskers with the aid of microwave irradiation. Antimony trichloride and thiourea are used as the starting materials and *N,N*-dimethylformamide (DMF) is chosen as the solvent. The strong complexing action between antimony trichloride and thiourea leads to the formation of the antimony–thiourea complex, which has already been well-studied previously.<sup>10b</sup> The decomposition of this complex with the inducement of microwave irradiation finally results in the formation of radial arrays composed of prismatic  $\text{Sb}_2\text{S}_3$  whiskers. This process is very convenient and efficient, free of any templates or crystal seeds, and the results are easily reproducible. It provides a novel one-pot solution-phase route that leads to the formation of 1D structural prismatic  $\text{Sb}_2\text{S}_3$  whiskers and their simultaneous assembly into radial arrays.

## Experimental Section

All the reagents were of analytical purity and were purchased from Shanghai Chemical Reagent Factory (China). In a typical procedure, 0.45 g of anhydrous  $\text{SbCl}_3$  and 0.45 g of thiourea were dissolved in 50 mL of DMF. Then, the mixture solution was placed in the microwave reflux system, and the reaction was performed under ambient air for 20 min. A microwave oven with 650-W power (Sanle General Electric Corp., Nanjing, China) was used in our experiments, and a refluxing system was connected with

\* Corresponding author. E-mail: jjzhu@nju.edu.cn. Fax: +86-25-3317761. Tel.: +86-25-3594976.

<sup>†</sup> State Key Laboratory of Coordination Chemistry, Nanjing University.

<sup>‡</sup> National Laboratory of Solid State of Microstructures, Nanjing University.

<sup>§</sup> Yangzhou University.

(1) (a) Devreese, J. T.; Evrard, R. P.; VanDoren, V. E. *Highly Conducting One-Dimensional Solids*; Plenum: New York, 1979. (b) Lieber, C. M.; Liu, J.; Sheehan, P. E. *Angew. Chem., Int. Ed. Engl.* **1996**, *35*, 687. (c) Lieber, C. M.; Wu, X. L. *Acc. Chem. Res.* **1991**, *24*, 170. (d) Dai, H.; Lieber, C. M. *Annu. Rev. Phys. Chem.* **1993**, *44*, 237.

(2) For reviews, see: (a) Patzke, G. R.; Krumeich, F.; Nesper, R. *Angew. Chem., Int. Ed.* **2002**, *41*, 2446. (b) Hu, J.; Odom, T. W.; Lieber, C. M. *Acc. Chem. Res.* **1999**, *32*, 435. (c) Lieber, C. M. *Solid State Commun.* **1998**, *107*, 607. (d) Yang, P.; Wu, Y.; Fan, R. *Int. J. Nanosci.* **2002**, *1*, 1.

(3) Rai-choudhury, P. *Handbook of Microlithography, Micromachining, and Microfabrication*; SPIE Press, IEEE: New York, 1999.

(4) (a) Levitt, A. P. *Whisker Technology*; Wiley-Interscience: New York, 1970. (b) Morales, A. M.; Lieber, C. M. *Science* **1998**, *279*, 208. (c) Duan, X.; Lieber, C. M. *Adv. Mater.* **2000**, *12*, 298. (d) Wu, Y.; Yang, P. *Chem. Mater.* **2000**, *12*, 605. (e) Shi, W. S.; Peng, H. Y.; Wang, N.; Li, C. P.; Xu, L.; Lee, C. S.; Kalish, R.; Lee, S. T. *J. Am. Chem. Soc.* **2001**, *123*, 11095. (f) Pan, Z. W.; Dai, Z. R.; Wang, Z. L. *Science* **2001**, *291*, 1947. (g) Chen, Y.; Ohlberg, D. A. A.; Medeiros-Ribeiro, G.; Chang, Y. A.; Williams, R. S. *Appl. Phys. Lett.* **2000**, *76*, 4004.

(5) For examples, see: (a) Martin, C. R. *Science* **1994**, *266*, 1961. (b) Routkevitch, D.; Bigioni, T.; Moskovits, M.; Xu, J. M. *J. Phys. Chem.* **1996**, *100*, 14037. (c) Xu, D.; Shi, X.; Guo, G.; Gui, L.; Tang, Y. *J. Phys. Chem. B* **2000**, *104*, 5061. (d) Jiang, X.; Xie, Y.; Lu, J.; Zhu, L.; He, W.; Qian, Y. *Chem. Mater.* **2001**, *13*, 1213.

(6) For examples, see: (a) Holmes, J. D.; Johnston, K. P.; Doty, R. C.; Korgel, B. A. *Science* **2000**, *287*, 1471. (b) Liu, S. W.; Yue, J.; Gedanken, A. *Adv. Mater.* **2001**, *13*, 656. (c) Jana, N. R.; Gearheart, L.; Murphy, C. J. *Chem. Commun.* **2001**, 617.

(7) Mane, R. S.; Lokhande, C. D. *Mater. Chem. Phys.* **2000**, *65*, 1 and the references therein.

(8) Wyckoff, R. W. G. *Crystal structure*, 2nd ed.; Wiley: New York, 1964.

(9) Mahanty, S.; Merino, J. M.; Leon, M. *J. Vac. Sci. Technol., A* **1997**, *15*, 3060.

(10) (a) Yu, S. H.; Shu, L.; Wu, Y. S.; Qian, Y. T.; Xie, Y.; Yang, L. *Mater. Res. Bull.* **1998**, *33*, 1207. (b) Yang, J.; Zeng, J. H.; Yu, S. H.; Yang, L.; Zhang, Y. H.; Qian, Y. T. *Chem. Mater.* **2000**, *12*, 2924. (c) Wang, H.; Zhu, J. J.; Chen, H. Y. *Chem. Lett.* **2002**, 1242. (d) Zheng, X.; Xie, Y.; Zhu, L.; Jiang, X.; Jia, Y.; Song, W.; Sun, Y. *Inorg. Chem.* **2002**, *41*, 455.

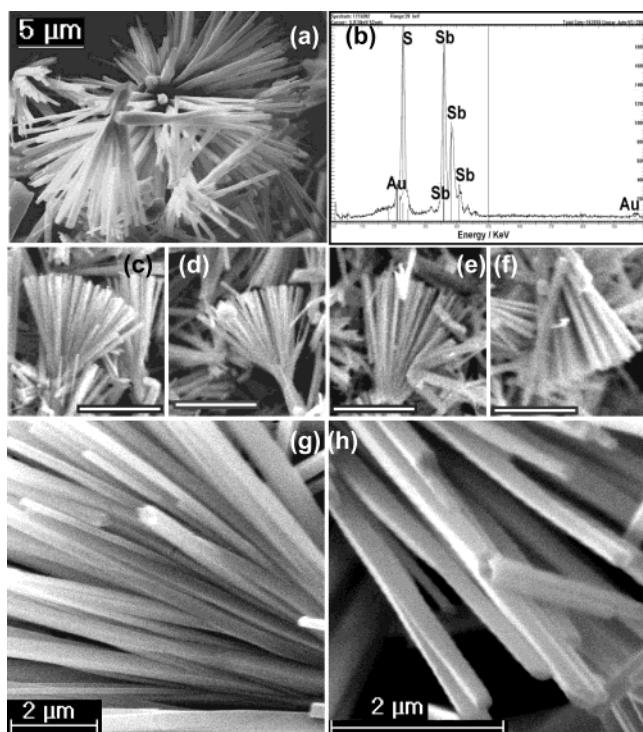


**Figure 1.** (a) Typical SEM image with low magnification revealing the overall morphology of several bunches of radial arrays composed of whiskers. (b) EDAX pattern of the  $\text{Sb}_2\text{S}_3$  whiskers shown in Figure 1a. (c–f) Several SEM images showing individual bunches of radial arrays. The length of the bars equals  $10\ \mu\text{m}$ . (g and h) SEM images with higher magnifications showing sectional images of radial arrays.

the microwave oven. The microwave oven followed a working cycle of 9-s on and 21-s off (30% power). At the end of the reaction, a great amount of black precipitate occurred. After cooling to room temperature, the precipitates were centrifuged, washed with DMF, distilled water, and absolute ethanol in sequence, and dried in air at room temperature. The final product was collected for characterizations.

Scanning electron microscopy (SEM) and energy-dispersive X-ray (EDAX) analysis patterns were taken on a JSM-6301F scanning electron microscope, operated at 20 kV. X-ray powder diffraction (XRD) measurements were performed on a Shimadzu XD-3A X-ray diffractometer with graphite monochromatized Cu K $\alpha$  radiation ( $\lambda = 0.154\ 18\ \text{nm}$ ) and a nickel filter. The acceleration voltage was 35 kV with a 150 mA current flux. Scatter and diffraction slits of 0.5 mm and collection slits of 0.3 mm were used. XRD patterns were taken of the powders attached to a glass slide, and data were collected in the  $2\theta$  range from  $10^\circ$  to  $65^\circ$ , with a scanning rate of  $4^\circ/\text{min}$  and a sample interval of  $0.02^\circ$ . The transmission electron microscopy (TEM) micrograph, selected area electron diffraction (SAED) pattern, and high-resolution transmission electron microscopy (HRTEM) micrographs were obtained by employing a JEOL-4000EX high-resolution transmission electron microscope with a 400-kV accelerating voltage. A conventional charge-coupled device video camera with a spatial resolution of  $768 \times 512$  pixels was employed to digitize the micrographs, which were then processed using Digital Micrograph software. The samples used for the TEM and HRTEM observations were prepared by suspending the dried sample in absolute ethanol in a sonication bath for 15 min. A drop of the sample suspension was then dropped onto a copper grid coated with a layer of amorphous carbon, and the copper grid was dried in air at room temperature.

## Results and Discussions

The dimensions and morphology of the product were characterized by SEM measurements. In a typical SEM image of the product, which is shown in Figure 1a, some bunches of radial arrays composed of straight and smooth

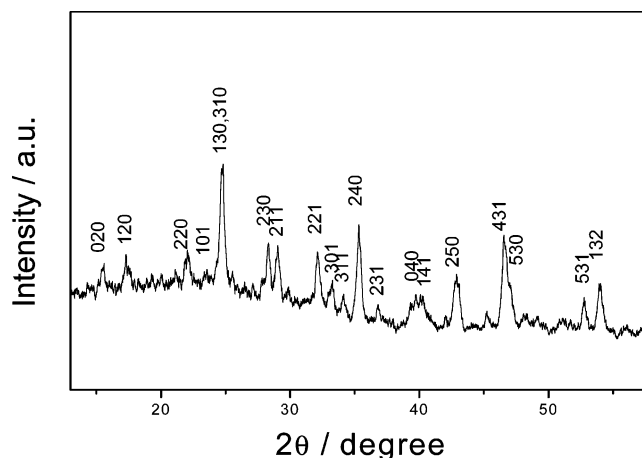


**Figure 2.** XRD pattern of the as-prepared  $\text{Sb}_2\text{S}_3$  powders.

whiskers with diameters of  $150\text{--}300\ \text{nm}$  and lengths of  $7\text{--}12\ \mu\text{m}$  can obviously be observed. The selected area EDAX analysis pattern (Figure 1b) confirms that the image in Figure 1a contains only antimony and sulfur atoms and the atomic ratio of Sb/S is calculated to be 1:1.47, which indicates the stoichiometric relation between Sb and S in this sample. Figure 1c–f shows the SEM images of some typical individual radial arrays. It is apparent that each array is made up of a bunch of regular whiskers that grow radially from one center to form a broomlike pattern. Some SEM images with higher magnifications (Figure 1g,h) recorded on sectional regions of a radial array reveal that each whisker has a fairly uniform diameter and appears to present a regular polygonal prismatic morphology.

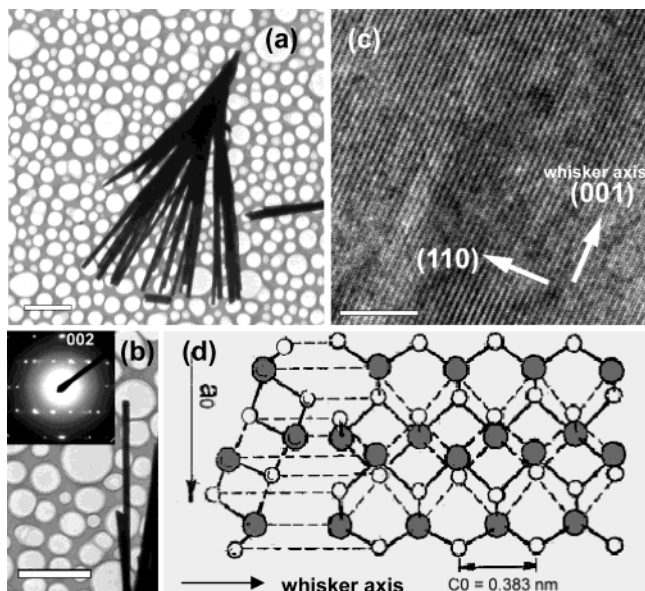
XRD measurements were carried out to determine the crystalline phase of the as-prepared powders. The XRD pattern of the product is shown in Figure 2. All the diffraction peaks can be indexed to be the pure orthorhombic phase for  $\text{Sb}_2\text{S}_3$ . The intensities and positions of the peaks match those data reported in the literature very well.<sup>11</sup> The cell parameters are calculated to be  $a = 11.179$ ,  $b = 11.280$ , and  $c = 3.826\ \text{\AA}$ , which are in good agreement with the literature values.<sup>11</sup> No peaks of any other phases are detected, indicating the high purity of the product.

Figure 3a shows a typical TEM image of a bunch of  $\text{Sb}_2\text{S}_3$  whiskers aligned radially to form a broomlike array. Figure 3b is the TEM image of an individual  $\text{Sb}_2\text{S}_3$  whisker with a diameter of  $\sim 180\ \text{nm}$ . The inset is a SAED pattern recorded on this whisker with a convergent electron beam, which indicates that this  $\text{Sb}_2\text{S}_3$  whisker presents a single-crystalline structure with a preferential 1D growth along the (001) crystal plane. HRTEM images recorded on individual  $\text{Sb}_2\text{S}_3$  whiskers provide further insight into their structures. The HRTEM image recorded on an interior part of a single  $\text{Sb}_2\text{S}_3$  whisker (Figure 3c) exhibits good crystallinity and clear lattice fringes. The interplanar spacing is measured to be about  $0.801\ \text{nm}$ , which corresponds to the (110) plane of the orthorhombic system of  $\text{Sb}_2\text{S}_3$ . The continuous (110) lattice fringes are parallel to the whisker axis. On the basis of the HRTEM observations, it is concluded that these  $\text{Sb}_2\text{S}_3$  whiskers preferentially grow along the (001) crystal plane. The illustration of the structure of an  $\text{Sb}_2\text{S}_3$  whisker is schematically shown in Figure 3d.

The formation process of the radial arrays of  $\text{Sb}_2\text{S}_3$  whiskers can be reasonably divided into two stages. In

(11) Joint Committee on Powder Diffraction Standards (JCPDS), No. 42-1393; International Center for Diffraction Data: Newton Square, PA, 1999.





**Figure 3.** (a) Typical TEM image of a bunch of  $\text{Sb}_2\text{S}_3$  whiskers aligned radially, forming a broomlike array. The length of the bar equals  $2\ \mu\text{m}$ . (b) TEM image of an individual  $\text{Sb}_2\text{S}_3$  whisker with a diameter of  $\sim 180\ \text{nm}$ . The inset is a SAED pattern recorded on this whisker. The length of the bar equals  $2\ \mu\text{m}$ . (c) A HRTEM image recorded on an interior part of an individual  $\text{Sb}_2\text{S}_3$  whisker. The length of the bar equals  $10\ \text{nm}$ . (d) The illustration of the structure of an  $\text{Sb}_2\text{S}_3$  whisker. The dark spheres represent S atoms and the bright spheres represent Sb atoms.

the first stage (nucleation stage), the antimony–thiourea complex dissolved in DMF underwent a microwave-induced decomposition process, leading to the rapid generation of  $\text{Sb}_2\text{S}_3$  nuclei. In the second stage (crystal growth stage), the in situ generated  $\text{Sb}_2\text{S}_3$  nuclei grew preferentially along the (001) crystal plane, which results in the formation of single-crystalline whiskers. It is noteworthy that because a bunch of whiskers grew radially from one nucleus simultaneously, radial arrays formed at the end of the crystal growth. Microwave irradiation played a critical role in both of the two stages mentioned previously. Microwaves are electromagnetic waves, containing both electric and magnetic field components.<sup>12</sup> In the case of a liquid-phase microwave reaction, a coupling between the oscillating electric field (2.45 GHz) and the permanent dipole moment of the molecules resulted in molecular rotations, which leads to rapid volumetric heating of the liquid phase. Such dielectric heating is capable of driving the thermal decomposition of the antimony–thiourea complex to produce  $\text{Sb}_2\text{S}_3$  nuclei. Compared with conventional heating methods, microwave dielectric heating presents a much more rapid and simultaneous nucleation due to the fast and homogeneous heating effects of microwaves. With microwave irradiation of reactants in polar solvents, temperature and concentration gradients can be effectively avoided, providing a uniform environment for the nucleation, which is very important to the final formation of uniform and regular whiskers. Microwave irradiation is also capable of inducing the preferential 1D growth of the  $\text{Sb}_2\text{S}_3$  crystals. One possible hypothesis of microwave-induced effects is the generation of localized high temperatures and pressures at the reaction sites to enhance the reaction rates in an

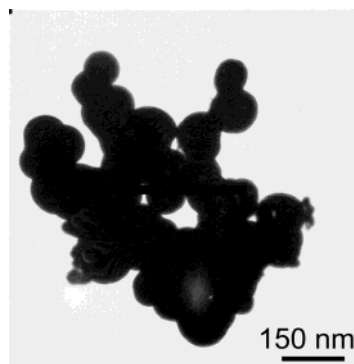


**Figure 4.** TEM image of  $\text{Sb}_2\text{S}_3$  powders prepared by refluxing the reactant mixture by means of conventional heating for 2 h. The powder XRD measurement shows that this sample is orthorhombic  $\text{Sb}_2\text{S}_3$ . The EDAX result shows that the Sb/S atomic ratio of this sample is 1:1.45.

analogous manner to that of ultrasound waves,<sup>13</sup> where both localized transient high pressures and temperatures are produced during reactions,<sup>14</sup> which is favorable for the 1D growth of  $\text{Sb}_2\text{S}_3$  crystals.<sup>10b,c</sup> It was observed that, after microwave heating for only 5 min, the temperature of the reactant mixture reached the boiling point of DMF ( $152.8\ ^\circ\text{C}$ ), and then the temperature of the boiling solution remained at  $153 \pm 1.5\ ^\circ\text{C}$ . The boiling solution remained transparent, and no powders appeared until 13 min of treatment. At 13 min, the precipitate of the  $\text{Sb}_2\text{S}_3$  powders was generated rapidly, and almost all the product was formed within only 4–5 s. If the time of treatment was further prolonged to 30, 60, or even 90 min, the yield did not increase anymore, and the dimension and morphology of the product was almost kept unchanged. We have also carried out the control experiments by refluxing the reactant mixture by means of conventional heating instead of microwave irradiation. It was found that the reaction rate greatly decreased and no regular whiskers were generated even after reflux for over 2 h. Instead, only quasi-spherical grains with submicrometer sizes were obtained (see Figure 4).

The choice of solvent is also of key importance to the formation of the radial arrays of  $\text{Sb}_2\text{S}_3$  whiskers. Herein, DMF was chosen because of four aspects of consideration. First, because anhydrous  $\text{SbCl}_3$  hydrolyzes strongly in aqueous solutions, nonaqueous solvents should be used. Second, DMF has good solubility to the precursors, providing a homogeneous medium for the microwave-induced nucleation. Third, DMF is an excellent susceptor of the microwave irradiation because of its high permanent dipole. Finally, and most important of all, DMF has a suitable boiling point and viscosity. We have also used some other solvents with a lower boiling point instead of DMF, such as ethanol, propanol, and tetrahydrofuran. In all these cases, only amorphous  $\text{Sb}_2\text{S}_3$  powders were obtained. Figure 5a is a typical TEM image of the  $\text{Sb}_2\text{S}_3$  powders prepared by choosing ethanol as the solvent. It is observed that this sample is composed of aggregated quasi-spherical particles with diameters of 25–40 nm. The results of the SAED and XRD measurements obviously confirm its amorphous nature. If some high boiling point solvents, such as ethylene glycol and triethylene glycol, were used,  $\text{Sb}_2\text{S}_3$  powders with a high crystallinity

(13) Komarneni, S.; Li, D.; Newalkar, B.; Katsuki, H.; Bhalla, A. S. *Langmuir* **2002**, *18*, 5959.

(14) (a) Suslick, K. S. *Ultrasound: Its Chemical, Physical and Biological Effects*; VCH: Weinheim, Germany, 1988. (b) Suslick, K. S.; Price, G. J. *Annu. Rev. Mater. Sci.* **1999**, *29*, 295 and the references therein.

(12) Galema, S. A. *Chem. Soc. Rev.* **1997**, *26*, 233 and the references therein.

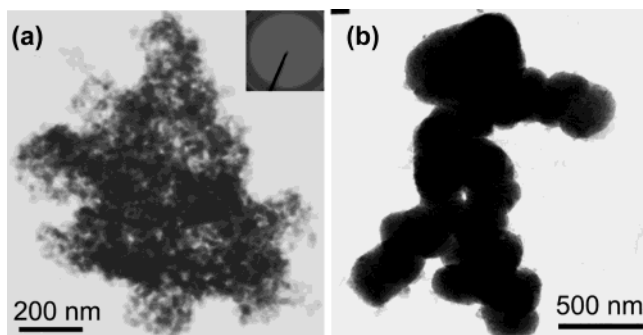


**Figure 5.** (a) TEM image of  $\text{Sb}_2\text{S}_3$  powders prepared by choosing ethanol as the solvent. The inset is the corresponding SAED pattern. The Sb:S ratio of this sample is calculated to be 1:1.40 according to the EDAX results. (b) TEM image of  $\text{Sb}_2\text{S}_3$  powders prepared by using triethylene glycol as the solvent. Powder XRD measurement shows that this sample is orthorhombic  $\text{Sb}_2\text{S}_3$ . The EDAX result shows that the Sb/S ratio is 1:1.48.

could be obtained. However, these products consisted of irregular grains. A typical TEM image of the  $\text{Sb}_2\text{S}_3$  sample prepared by using triethylene glycol as the solvent is shown in Figure 5b. In this case, because the viscosities of these solvents are much higher than that of DMF, the prefer-

ential 1D growth of the  $\text{Sb}_2\text{S}_3$  whiskers is inhibited and, thus, no whiskerlike products are obtained.

### Conclusion

In summary, a microwave-assisted solution-phase approach to produce radially aligned prismatic  $\text{Sb}_2\text{S}_3$  whisker arrays has been successfully established. It is a convenient one-pot method without using any templates or crystal seeds and has great potential in industrialized high-volume production. The extension of this approach may open fascinating possibilities for the fabrication and assembly of other V–VI group chalcogenide whisker arrays with wide applications in various kinds of thermoelectric and optoelectronic devices.

**Acknowledgment.** This work is supported by the National Natural Science Foundation of China (Grant 50072006 and 90206037), the Jiangsu Advanced Science and Technology Program of the People's Republic of China (BG 2001039) and "863" Project (No. 2003AA302740). The authors are also grateful to Mr. Jianmin Hong from Modern Analytic Center at Nanjing University for extending his facilities to us.

LA0351865